We are IntechOpen, the world's leading publisher of Open Access books Built by scientists, for scientists

6,900
Open access books available

186,000
International authors and editors

200M
Downloads

Our authors are among the

154
Countries delivered to

TOP 1%
most cited scientists

12.2%
Contributors from top 500 universities

CLARIVATE ANALYTICS
BOOK CITATION INDEX
INDEXED

WEB OF SCIENCE™

Selection of our books indexed in the Book Citation Index
in Web of Science™ Core Collection (BKCI)

Interested in publishing with us?
Contact book.department@intechopen.com

Numbers displayed above are based on latest data collected.
For more information visit www.intechopen.com

2

Artificial Photosynthesis from a Chemical Engineering Perspective

Bahar Ipek and Deniz Uner
Middle East Technical University,
Turkey

1. Introduction

Green plants and photosynthetic bacteria are responsible for storing solar energy in chemical bonds via photosynthesis. Photosynthesis is not only the major source of food, fuel and oxygen on earth, but it is also the key player in the global carbon cycle by converting 120 gigatonnes of carbon per year.

Conversion of solar energy into chemical energy through utilization of inorganic materials by photocatalytic CO_2 reduction; which is also known as '*Artificial Photosynthesis*' is the next challenge for a sustainable development. In the present state-of-the art artificial photosynthesis processes, nature is so far mimicked only to the extent that CO_2 is reduced by water to valuable 1- carbon chemicals, not to the multi-carbon equivalents of glucose or cellulose yet. Although mimicking nature is viable by photocatalytic means, enhancing photocatalytic CO_2 reduction rates is vital in order to achieve artificial photosynthesis in industrial scales. To illustrate the gap between photosynthetic and photocatalytic rates, we will compare the turnover frequencies of water oxidation process below.

Water oxidation is the key step both in photocatalysis and photosynthesis for being the carbon free hydrogen source and also for providing oxygen for the oxygen consuming organisms. Completion of an S cycle taking place in a Mn_4 cluster which is responsible for water oxidation was reported to last for 1.59 ms in order to produce one molecule of oxygen at that one particular site (Haumann et al., 2005). In other words, molecular oxygen is produced in photosynthesis, with a turn over frequency of 630 molecule/site/s. On the other hand, typical rates of photocatalytic synthesis of hydrocarbons are of the order of 30-μmoles/g cat/h, (Ozcan et al., 2007; Uner et al., 2011) which amounts to $1.11*10^{-5}$ molecule/site/s if the typical surface areas of 45 m^2/g cat and typical site densities of 10^{15}/cm^2 are used. Of course the remarkable rates of 9 μmoles of O_2/cm^2/s (Kanan & Nocera, 2008), giving a turn over frequency of 5400 molecule/site/s for an oxygen evolving cobalt- phosphate catalyst operating at neutral water is keenly followed by the academic community. Considering the huge gap between photosynthetic and photocatalytic rates reported above, one can easily claim that there is room for further investigation and development in photocatalytic CO_2 reduction systems.

It is also important to see the thermodynamic energy demand of the some of the reactions between CO_2 and H_2O. For this, a number of products are chosen and the standard Gibbs free energy of formation values are listed in Table 1.1 for comparison. The interesting

observation that we make in this table is the following: when compared per mole of hydrocarbon formed, the Gibbs free energies of formation increase with increasing carbon chain length. But when the Gibbs free energy formation values are normalized per mole O_2 formed, one can compare the energy demand of the reactions on a common basis. A close examination of the data in the last column reveals the fact that energetically almost all of the reactions are similar. The second conclusion we can arrive at is that once the water splitting reaction is possible, the formed hydrogen can drive the subsequent reduction reactions, almost spontaneously.

Reaction	ΔG_f (kJ/mol HC product)	ΔG_f (kJ/mol O_2)
$CO_2 + 2H_2O \Rightarrow CH_4 + 2\,O_2$	801.0	400.5
$CO_2 + 2H_2O \Rightarrow CH_3OH + 1\frac{1}{2}\,O_2$	689.2	459.5
$2\,CO_2 + 3H_2O \Rightarrow C_2H_5OH + 3\,O_2$	1306.6	435.5
$H_2O + CO_2 \Rightarrow 1/6\,C_6H_{12}O_6 + O_2$	2880.0	480.0
$H_2O \Rightarrow H_2 + \frac{1}{2}\,O_2$	228.6	457.2

Table 1.1. The thermodynamics of the reactions involved in carbon dioxide reduction

2. Photosynthesis

2.1 Overview

Photosynthesis is the world's most abundant process with an approximate carbon turnover number of 300- 500 billion tons of CO_2 per year. In this vital process, green plants, algae and photosynthetic bacteria are converting CO_2 with water into carbohydrates and oxygen (in oxygenic photosynthesis), both of which are essential for sustaining life on earth. Oxygenic photosynthesis is believed to be started 2.5 billion years ago by the ancestors of cyano bacteria. In this remarkable process, energy need for converting stable compounds (CO_2 and H_2O) into comparably less stable arranged molecules ($(CH_2O)_n$ and O_2) is supplied from solar energy in which highly sophisticated protein complexes embedded in an internal chloroplast membrane (called thylakoid membrane) are major players.

$$6CO_2 + 12\,H_2O + Light\ Energy \rightarrow C_6H_{12}O_6 + 6O_2 + 6H_2O$$
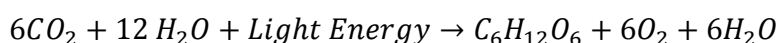
$$\Delta G^0 = 2880\ kJ\ /mol\ C_6H_{12}O_6$$

Harnessing solar energy into chemical bonds in this process is achieved by light absorption and sequential electron and proton transport processes in which a great deal of number of light harvesting pigments, protein complexes and intermediate charge carriers are involved. CO_2 is being reduced with the indirect products of water oxidation; supplying required energy in the form of redox free energy (from NADPH) and high energy Pi bonds (from ATP).

Overall process can be shown in the reaction scheme below where D: electron donor, A: electron acceptor and T: energy trap (Govindjee, 1975).

Water oxidation: $D^+ \cdot T \cdot A + \frac{1}{2}H_2O \rightarrow D \cdot T \cdot A + \frac{1}{4}O_2 + H^+$

$NADP^+$ reduction: $D^+ \cdot T \cdot A^- + \frac{1}{2}NADP^+ + H^+ \rightarrow D^+ \cdot T \cdot A + \frac{1}{2}NADPH + \frac{1}{2}H^+$

Cyclic Photophosphorylation: $D^+ \cdot T \cdot A^- + ADP + P_i \rightarrow D \cdot T \cdot A + ATP$

CO_2 reduction: $CO_2 + 2\,NADPH + 3\,ATP \rightarrow (CH_2O) + 2NADP^+ + 3\,ADP + 3P_i$
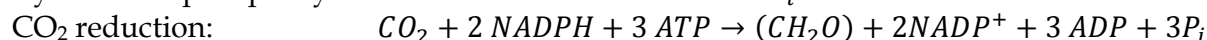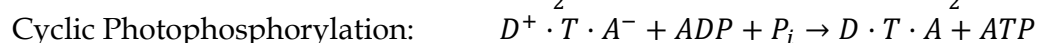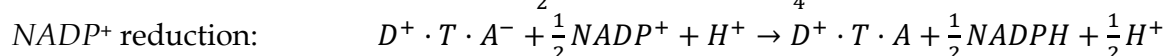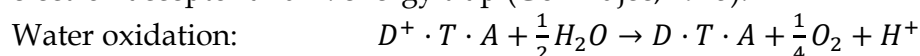
2.2 Reactions

Photosynthesis includes a series of photophysical, photochemical and chemical reactions realized by highly sophisticated protein complexes, energy carriers and enzymes. With all the complexity of their mechanisms, reactions involved in photosynthesis are mainly divided into two stages: (i) light dependent reactions including water oxidation and chemical energy generation through electron and proton transport and (ii) light independent reactions including CO_2 fixation, reduction and regeneration of ribulose 1,5 biphosphate (Calvin Cycle).

2.2.1 Light induced reactions

The light induced reactions occur in a complex membrane system (thylakoid membrane) via electron transfer through light induced generation of cation- anion radical pairs and intermediate charge carriers such as plastoquinone, plastocyanin and ferrodoxin. Light dependent reactions in green plants follow a Z scheme which was first proposed by Hill & Bendall, 1960 (Figure 2.1). In this scheme, light energy is absorbed by light harvesting molecules and funneled to two special reaction center molecules; P680 and P700 which are acting as major electron donors in PS II and PSI respectively. Electron transport from PSII to PS I is realized by intermediate charge carriers and electron need of P680$^+$ (strong oxidant with $E^0 = 1.1$ eV) in PSII is compensated from water molecules (water oxidation).

Electron transport through thylakoid membrane and water oxidation reactions results in a proton concentration gradient across the thylakoid membrane. Energy created by proton electrochemical potential resulting from this proton gradient is used by ATP synthase to produce ATP from ADP and Pi. The net reaction in light dependent reaction system is the electron transport form a water molecule to a NADP$^+$ molecule with the production of ATP molecules (Figure 2.2).In this complex electron transport system, PS II alone is composed of more than 15 polypeptides and nine different redox components including chlorophylla and b, pheophytin, plastoquinone.
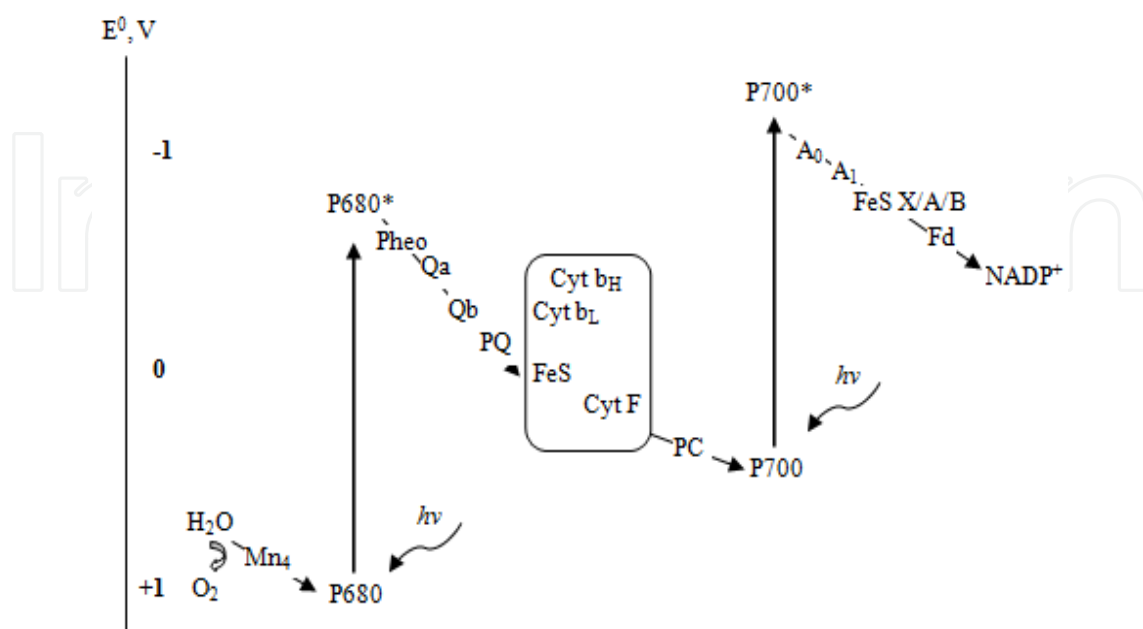

Fig. 2.1. Z scheme electron transfer in terms of redox potentials (Ke, 2001)

Photosystem II is the only protein complex with the capability of oxidizing water into O_2 and protons. In PS II, water is oxidized with an Oxygen Evolving Complex whose components are revealed to be in the form of Mn_4CaO_5 (Umena et al., 2011). This inorganic core oxidizes two water molecules in Kok cycle, comprised of five oxidation states (S states) of PSII donor site. In this model, oxygen formation requires successive four light flashes for four-electron and four-proton release. Recently, presence of an intermediate S_4' state and kinetics of completion of final oxidation cycle responsible for O- O bond formation was revealed with time resolved X ray study of Haumann et al. (Figure 2.3) (Haumann et al., 2005).
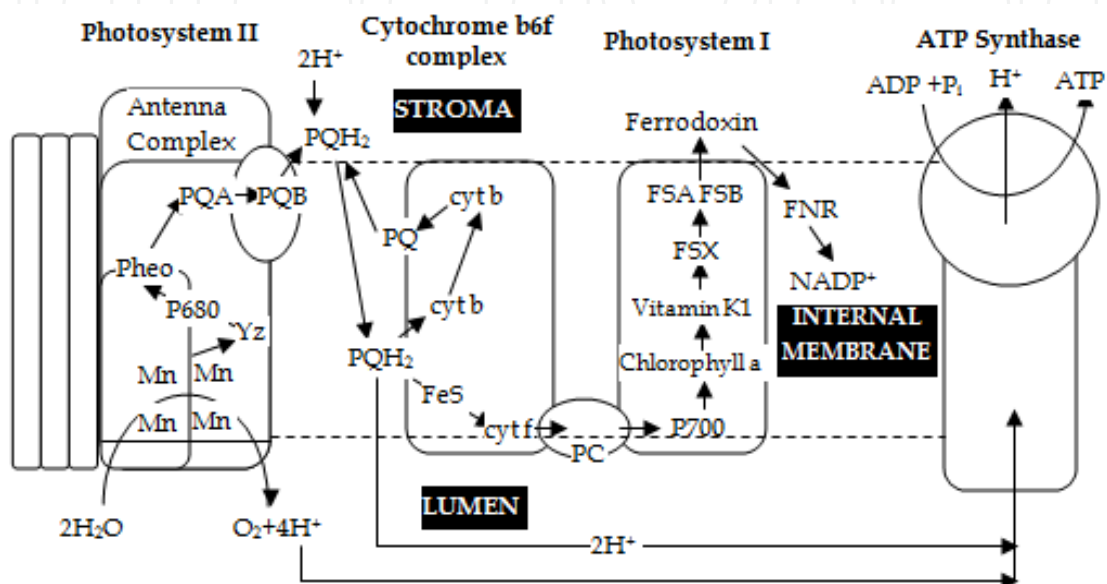

Fig. 2.2. Schematic illustrations of electron and proton transport processes and ATP synthesis in light dependent reactions (Hankamer et al., 1997)
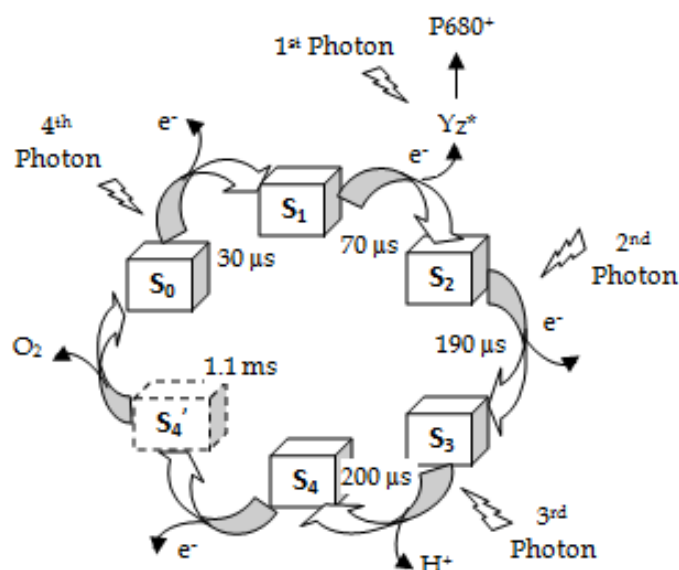

Fig. 2.3. Extension of classical S state cycle of the manganese- calcium complex (Haumann et al., 2005)

This high energy requiring water oxidation reaction with four- proton, four- electron extraction and an oxygen- oxygen bond formation (with a standard free energy requirement of 312 kJ/mol of O_2) necessitates the regeneration of the oxygen evolving complex at every half an hour in order to repair the damage caused by the oxygen production (Meyer, 2008).

In electron transfer from the oxygen evolving complex (OEC) to P680$^+$ molecule, tyrosine (Y_z*) acts as intermediate electron carrier. Protons evolved from OEC are deposited in lumen phase contributing proton concentration gradient (ΔpH) mentioned in ATP synthesis part. Excited electron upon light absorption is transferred to the cytochrome b6f complex through a pheophytin, a tightly bound phylloquinone (Q_A) and a mobile phylloquinone (Q_B). Subsequently reduced phylloquinol (PQH_2) (reduced with electrons from P680* and two protons from stromal phase) releases two additional protons into lumen phase as it binds to cyctochrome b6f complex after diffusion through thylakoid membrane. Electron transfers from cyctochrome b6f complex to PS I (through lumen phase) and from PS I to NADP$^+$ molecule (through stromal phase) are achieved by plastocyanin and ferrodoxin respectively. ATP synthesis reaction in light dependent reactions is driven by the proton electrochemical and charge potential across the membrane resulted from proton concentration difference and charge separation during illumination respectively. NADPH and ATP molecules produced as such are used as energy and proton sources in carbon dioxide reduction reactions in Calvin Cycle.

2.2.2 Dark reactions

The reactions that do not involve solar energy directly are somewhat roughly called the dark reactions. These reactions take place in outer space of thylakoid membrane which is also known as stromal phase. CO_2 enters the leaf structure through small holes called stomata and diffuses into stromal phase in the chloroplast where it is being reduced with reactions in series that are catalyzed by more than ten enzymes. Driving force for the reduction reaction is supplied from NADPH and ATP molecules; hence, the *'catalytic'* reaction sequence does not require light as an energy source and called as light independent reactions. However, recent findings indicate light activation of enzymes due to regulatory processes (reductive pentose phosphate).

Melvin Calvin and his collaborators were the first to resolve the photosynthetic CO_2 reduction mechanism with studies involving radioactively labeled CO_2. The Calvin Cycle, also known as reductive pentose phosphate pathway consists of three sections:

1. CO_2 fixation by carboxylation of rubilose 1,5- bisphosphate to two 3-phosphoglycerate molecules,
2. Reduction of 3-phosphoglycerate to triose phosphate, and
3. Regeneration of rubilose 1,5- bisphosphate from triose phosphate molecules (Figure 2.4).

The key reaction in photosynthetic CO_2 reduction is the fixation of a CO_2 molecule to rubilose 1,5- bisphosphate to two phosphoglycerate molecules with a standard free energy of -35 kJ/mol indicating its irreversibility. This reaction is catalyzed with the Ribulose biphosphate Carboxylase/Oxygenase (RubisCO) enzyme which is one of largest enzymes in nature with its 8 large, 8 small subunits (with molecular weights changing from 12 to 58 kDa). This enzyme also catalyzes a side reaction, oxygenation, to give a 3-phospho glycerate and a 2- phosphoglycolate instead of two 3- phosphoglycerates for CO_2 fixation. Although

oxygenation occurs with a ratio of 1:4 to 1:2 (oxygenation : carboxylation), oxygenation decreases as CO_2 concentration in the atmosphere is increased. This regulatory measure of photosynthesis is worth appreciation.
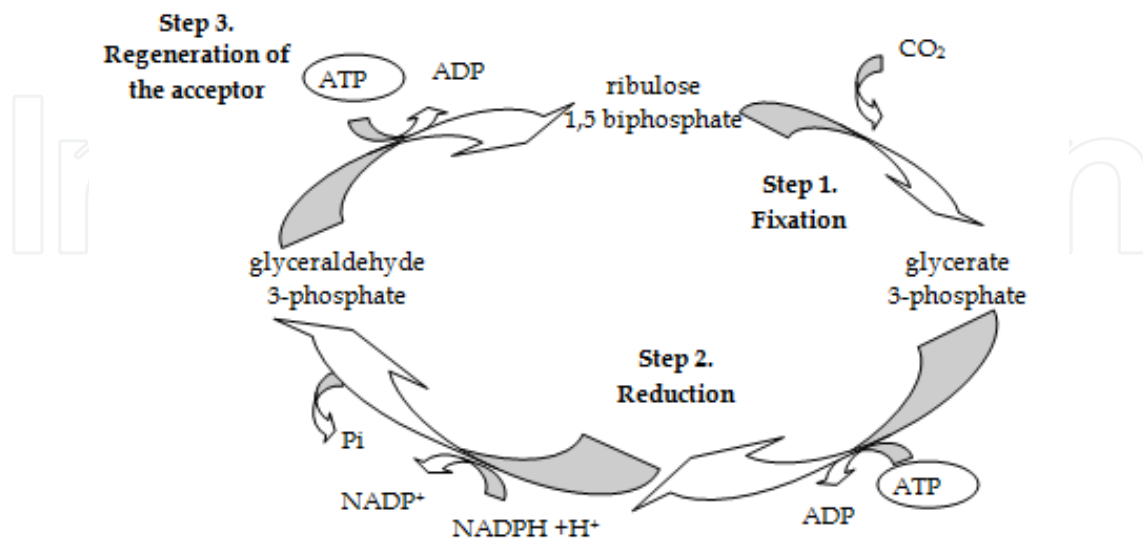

Fig. 2.4. The Calvin Cycle

In carboxylation reaction catalyzed by RubisCO, rubilose 1,5- bisphosphate (RuBP) accepts CO_2 to form a keto intermediate after keto-enol isomerization (Figure 2.5). For the synthesis of glyceraldehydes 3- phosphates, firstly 3- phosphoglyerates are phospholyrated to 1,3- bisphosphoglycerate with phosphoglycerate kinase enzyme. Afterwards, 1,3- biphosphoglycerate is reduced with NADPH to glyceraldehydes 3- phosphate with glyceraldehydes phosphate dehydrogenase enzyme. Redox potential difference between the aldehyde and carboxylate is overcome with the consumption of ATP (Figure 2.6).
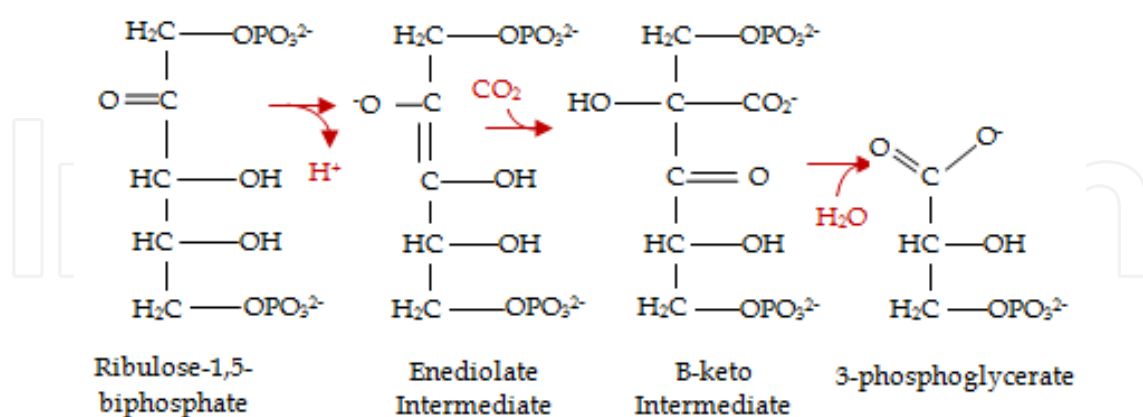

Fig. 2.5. Reaction sequence of carboxylation of RuBP by RubisCO (Diwan, 2009)

After production of glyceraldehyde 3- phosphates, out of six aldehydes produced by fixation of three CO_2 molecules, five of them are used in regeneration of three RuBP molecules together with ATP consumption. Remaining one molecule of glyceraldehyde 3- phosphate is transported into the cytosol for utilization in glucose synthesis.
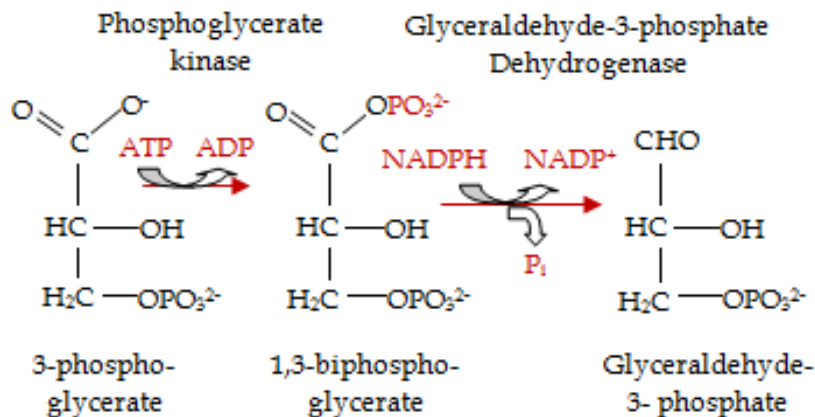
Fig. 2.6. Conversion of 3- Phosphoglycerate to triose phosphate (Diwan, 2009)

2.3 Transport processes

The vesicular thylakoid membrane structure defines a closed space separating outside water phase (stromal phase) and inside water phase (lumen phase). CO_2 fixation reactions occur in the stromal phase while majority of light dependent reactions are realized in the complex membrane system with embedded protein complexes and intermediate charge carriers.

As mentioned in light dependent reactions, electron and proton transport processes through protein complexes and intermediate charge carriers like plastoquinone, plastocynanin and ferrodoxin molecules play an important role in controlling photosynthetic rates. Within a protein complex such as PSII or cytochrome bf complex, electron transfer and pathway is controlled by polypeptide chains of the protein. However between protein complexes, electron transfer via electron carriers is controlled by distance and free energy. Below, electron and proton transport processes taken place in light dependent reactions are illustrated with particle sizes of protein complexes given by Ke, 2001.
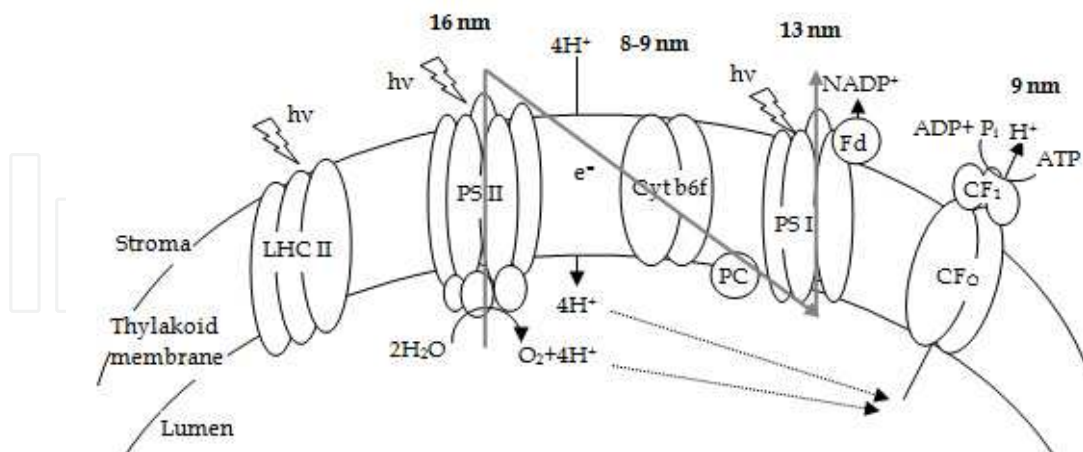

Fig. 2.7. Distribution of photosynthetic complexes in thylakoid membrane and the corresponding Z scheme (Ke, 2001)

Presence of the membrane affects reaction rates in an aspect that it limits electron and proton transport to two dimensions which increases the random encounters. Furthermore, electron transport reactions and special structure and orientation of the membrane and protein complexes contribute to a proton electrochemical potential difference which drives

ATP synthesis reaction; i.e., plays a significant role in energy supply of photosynthesis. The proton electrochemical potential difference across the membrane is created by two main contributions; i. proton concentration gradient (pH difference), and ii. electric potential difference.

The processes contributing *proton concentration difference (ΔpH)* across the membrane can be listed as below:

1. Proton release to the lumen phase as a consequence of water oxidation reaction at PS II.
2. Proton uptake from stromal phase for PQ reduction.
3. Proton release into lumen phase during PQH_2 oxidation at cytochrome b6f complex.
4. $NADP^+$ reduction at stromal phase.

On the other hand, vectoral electron transfer process in PS II and PS I initiated by photon absorption could be accounted as the reason for *electric potential difference (ΔΨ)*. Whitmarsh & Govindjee, 1999 gave the proton electrochemical potential difference with Equation (1).

$$\Delta\mu_{H+} = F\Delta\Psi - 2.3RT\Delta pH \tag{1}$$

Where F is the Faraday constant, R is the ideal gas constant and T is temperature in Kelvin. They reported that although electric potential difference can be as large as 100 mV, pH difference has a dominating effect in overall electrochemical potential. For a pH difference of 2 (with inner pH 6 and outer pH 8, ΔpH equivalent to 120 mV), the free energy difference across the membrane is about -12 kJ/mol of proton.

In photosynthesis, fastest reactions taking place are the photophysical reactions like light absorption and charge separation in picoseconds orders. They are followed by rapid photochemical processes like electron transfer reactions and with slower biochemical reactions like water splitting and CO_2 reduction.

Since photosynthesis is a series of reactions including photophysical, photochemical and chemical reactions, reaction rates of particular reactions are dependent upon transfer rates of reaction intermediates like electrons or protons. In Figures 2.8 and 2.9, electron transfer times in PS II and PS I are given to illustrate characteristic times of different processes.
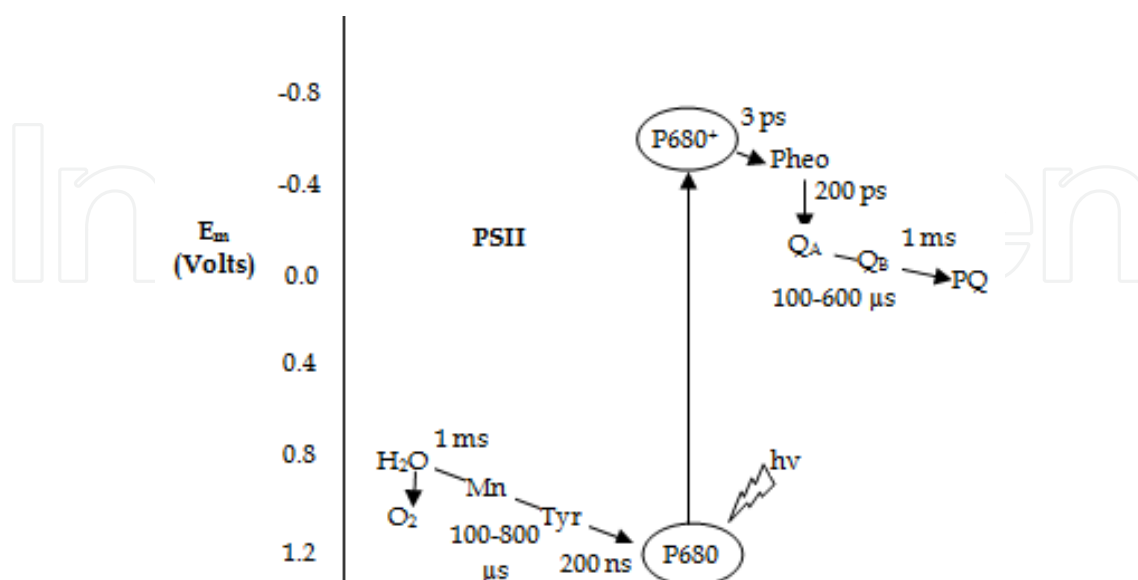

Fig. 2.8. PS II electron transport pathways and transfer times with midpoint potentials of electron carriers (Whitmarsh & Govindjee, 1999)
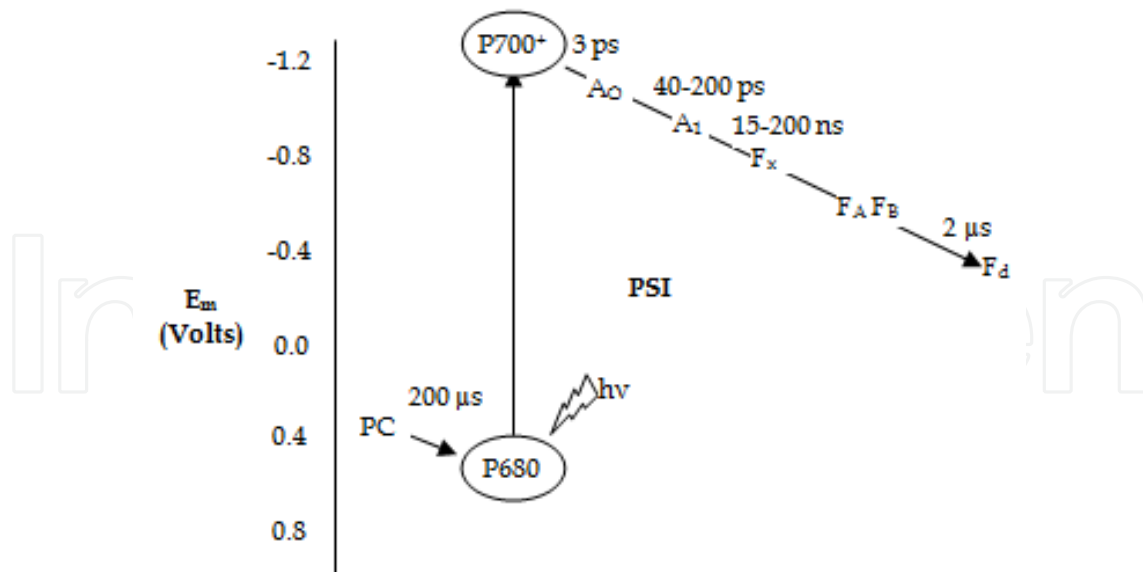
Fig. 2.9. PS I electron transport pathways and transfer times with midpoint potentials of electron carriers (Whitmarsh & Govindjee, 1999)

Water oxidation and CO_2 reduction reactions are the slowest processes in photosynthesis. S-cycle taking place in PS II for water oxidation is completed with a total of 1.59 ms, which is equivalent to production of 630 molecule of O_2/site/s. On the other hand, turnover frequency given for a subunit of RubisCO for CO_2 reduction is given as 3.3 s^{-1} (Heldt, 2010), which is much slower than oxygen evolution. Average photosynthesis rate of a sunflower was given as 13.5 µmol/m^2/s by Whittingham, 1974 and as 12 µmol/m^2/s for Brassica pods with an internal CO_2 concentration of 292 ppm by Singal et al., 1995 where rate of dark CO_2 fixation was given as 400 nmol/ mg protein/h.

In Table 2.1, time characteristics are unraveled for photosynthesis and artificial photosynthesis which indicates similarity in photochemistry but significant difference in time characteristics of chemical reactions.

Photosynthesis		Artificial Photosynthesis (on TiO_2)	
Charge carrier generation	ps	Charge carrier generation	ps
Charge trapping	ps-ns	Charge trapping	10 ns
Electron transport	ns- µs	Interfacial charge transfer	100 ns
Water oxidation	1.59 ms	Water oxidation	670 ms[a]
CO_2 reduction	300 ms	CO_2 reduction	14950 s[b]

Table 2.1. Time characteristics of major processes realized in photosynthesis and artificial photosynthesis

a. Oxygen evolution with cobalt ITO electrode (Kanan & Nocera, 2008)
b. Considering 200 µmole/g_{cat}/h activity and 50 m^2/g_{cat} and 10^{15} sites/cm^2

3. Artificial photosynthesis

Since the pioneering work of Inoue et al., 1979, CO_2 is being reduced with H_2O photocatalytically to mainly one carbon molecules like methane and methanol in the

presence of a photo-activated semiconductor. Electrons, generated upon illumination of the semiconductor, are trapped at the electron trap centers and utilized directly in reduction centers without a complex transportation system involving intermediate charge carriers. Similarly holes, generated upon illumination are utilized in oxidation reactions on the catalyst surface. Since photocatalysis lacks a specialized transportation system for generated electrons and holes, majority of the charge carriers recombine at the catalyst surface or in the bulk volume of the catalyst, lowering photocatalytic rates. (Figure 3.1)

Semiconductors, having a band gap, ensure a life-time for generated electrons and holes; however, this lifetime is limited to 10^{-7} s, which is the characteristic time of recombination (for bare TiO_2) (Carp et al., 2004). In order to increase this lifetime of photo-generated electrons and holes, some modifications on materials such as metal addition to semiconductors (Anpo et al., 1997, Tseng et al., 2002, Ozcan et al., 2007) or formation of solid-solid interfaces in composite catalysts (Chen et al., 2009, Woan et al., 2009) were proposed in literature.

Metal addition to semiconductors is suggested to show charge separation effect on photocatalysis by the Schottky Barrier Formation. When metals are brought into contact with semiconductors, electrons populate on metals if Fermi level of the metal is lower than the conduction band of the semiconductor. Hence, metals act like 'charge carrier traps', increasing lifetime of electron hole pairs with charge separation effect.
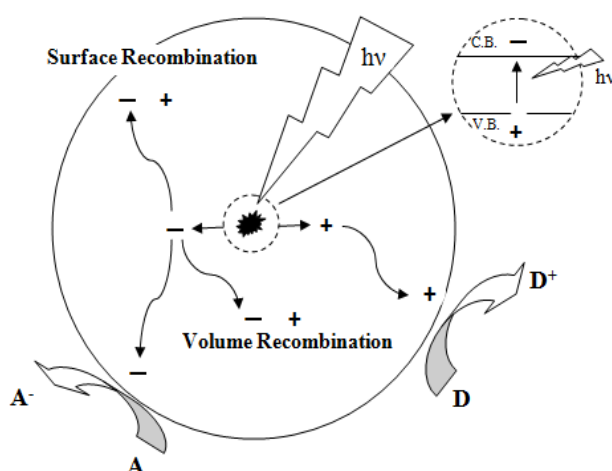

Fig. 3.1. Illustrating scheme of electron/hole pair generation and realization of redox reactions in photocatalysis

The other modification that can hinder recombination of generated electrons and holes is formation of solid-solid interfaces in composite photocatalysts having different band gap energies. To illustrate; commercial TiO_2 catalysts; Degussa P-25, is composed of anatase and rutile crystal phases of TiO_2, having band gap energies of 3.2 eV and 3.0 eV respectively. Mixed phase TiO_2, tends to exhibit higher photocatalytic activity than pure phases, because it allows transfer of the photogenerated electron from rutile to anatase, resulting in charge separation (Carp et al., 2004, Chen et al., 2009).

In photocatalysis, reduction and oxidation reactions occur at similar sites on the same catalyst surface. There are no different reaction centers with certain distances apart.

The half reactions of the photosynthesis; water oxidation and CO_2 reduction, are also realized in photocatalysis.

$$semiconductor \xrightarrow{hv} e^- + h^+$$

$$2H_2O + 4h^+ \rightarrow O_2 + 4H^+$$

$$CO_2 + 6H^+ + 6e^- \rightarrow CH_3OH + H_2O$$

$$CO_2 + 8H^+ + 8e^- \rightarrow CH_4 + 2H_2O$$
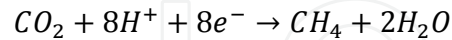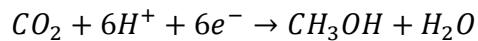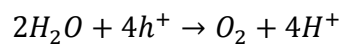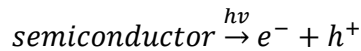
In photocatalysis; surface adsorbed species should have appropriate redox potentials regarding flat band positions of the semiconductor for thermodynamic favorability of the reactions, or vice versa. It required that; semiconductors should have conduction bands located at a more negative potential than the reduction potential of CO_2 to hydrocarbons, and valence bands located at a more positive potential than the oxidation potential of H_2O. In Table 3.1 oxidation and reduction reactions taking place in photocatalytic CO_2 reduction is listed with their electro-potentials at pH=7, vs NHE. In order to provide thermodynamic favorability, large band gap semiconductors such as TiO_2 are mostly utilized in photocatalytic CO_2 reduction reactions which render UV light illumination obligatory for photo-activation of the catalysts. Visible light utilization in carbon dioxide reduction is the ultimate goal in photocatalytic studies for a complete carbon free energy generation. There are material modification studies in literature conducted for efficient visible light utilization such as dye sensitization (Ozcan et al., 2007) and anion doping (Asahi et al., 2001).

Reactions	E^0 (V)
$2H_2O + 4h^+ \rightarrow O_2 + 4H^+$	+0.82
$CO_2 + 2H^+ + 2e^- \rightarrow HCOOH$	-0.61
$CO_2 + 2H^+ + 2e^- \rightarrow CO + H_2O$	-0.52
$CO_2 + 4H^+ + 4e^- \rightarrow HCHO + H_2O$	-0.48
$CO_2 + 6H^+ + 6e^- \rightarrow CH_3OH + H_2O$	-0.38
$CO_2 + 8H^+ + 8e^- \rightarrow CH_4 + 2H_2O$	-0.24

Table 3.1. Half cell reactions and their electro-potentials at pH=7 vs NHE (Jitaru, 2007)

One disadvantage of the realization of reduction and oxidation reactions at the same surface is the interaction between reactants on the surface. In one of the gas phase photocatalytic CO_2 reduction experiments realized on Cu/TiO_2 surfaces, when Langmuir- Hinshelwood surface reaction mechanism was selected with competitive adsorption of H_2O and CO_2, it was found that adsorption constant of H_2O dominates that of CO_2 (Wu et al., 2005) indicating that surface is mainly covered with water.

Presence of that much of water on TiO_2 surface would inhibit CO_2 activation ($CO_2+e^-\rightarrow CO_2^{\bullet-}$ E^0_{redox}= -1.9 V vs. NHE at pH 7), which is considered as the essential step in CO_2 reduction (Solymosi & Tombacz, 1994), by oxidizing defect structure of CO_2. Electron affinity of CO_2 molecule is related to the position of lowest unoccupied molecular orbital of CO_2 and conduction band of TiO_2, assuming that electron is transferred from excited state of TiO_2 (Ti^{+3}-O^-) to CO_2. A decrease in lowest unoccupied molecular orbital (LUMO) of CO_2 was reported with lower bond angles that could result from the interaction of the molecule with the surface (Freund & Roberts, 1996). According to Indrakanti et al., 2009, CO_2 gains electrons from oxygen deficient TiO_2 via the formation of bent CO_2 molecules near Ti^{+3} sites, whereas electron transfer is not favorable with defect free TiO_2 due to high LUMO of CO_2.

Initial photocatalytic carbon dioxide reduction rates from literature were summarized in Table 3.2. In those studies, carbon dioxide is reduced with water on the same catalyst surface in a batch reactor system.

Results presented at the table and in photocatalytic carbon dioxide reduction studies in general indicated very low carbon dioxide reduction yields when compared to photosynthetic and even to the catalytic carbon dioxide reduction yields. To illustrate, methanol was reported to be produced with a rate of 220 000 $\mu mol/g_{cat}/h$ with a $Cu/ZnO/Al_2O_3$ catalyst at 45 bar and 250 °C (Sahibzada et al., 1998). For a more proper comparison of catalytic and photocatalytic reduction rates, the results should be evaluated at the same conditions; i.e., at the same temperature and pressure. By this way, one could reveal the 'photocatalytic' effect in carbon dioxide reduction mechanism. Since catalytic carbon dioxide hydrogenation rate data are not available at ambient conditions, the comparison was based on the kinetic models of methanol synthesis on copper surfaces.

BATCH REACTORS					
GAS PHASE			*LIQUID PHASE*		
Photocatalyst	**Initial Rates ($\mu mol*gcat^{-1}*h^{-1}$)**		**Photocatalyst**	**Initial Rates ($\mu mol*gcat^{-1}*h^{-1}$)**	
	CH_4	**CH_3OH**		**CH_4**	**CH_3OH**
TiO_2 (Anpo & Chiba, 1992)	0,11	0,02	TiO_2 (Dey et al., 2004)	5,94	
JRC TiO_2 (Anpo et al., 1995)	0,17		TiO_2 (Degussa P25) (Tseng et al., 2002)		6,37
Cu/TiO_2 (Yamashita et al., 1994)	0,013	0,0015	Cu/TiO_2 (Tseng et al., 2002)		19,75
Ti-SBA-15 (Hwang et al., 2005)	63,60	16,62	TiO_2/SBA-15 (Yang et al., 2009)		627
Ti-MCM-48, (Anpo et al., 1998)	4,5	1,5	Cu/TiO_2/SBA-15 (Yang et al., 2009)		689,7
Pt/ Ti-MCM-48 (Anpo et al., 1998)	7,5	0,48	TiO_2 anatase (Koci et al., 2009)	0,38	0,045
TiO_2 (Kitano et al., 2007a)	0,2	0,003	Ag/ TiO_2 (Koci et al., 2010)	0,38	0,075
Ex-Ti-oxide/ Y-zeolite (Anpo et al., 1997)	4,2	2,4	TiO_2 (Kaneco et al., 1998)	0,72	
Pt TiNT (Zhang et al., 2009)	0,07		Rh /TiO_2 /WO_3 (Solymosi & Tombacz, 1994)		2,7
$CdSe/Pt/TiO_2$ (C.J. Wang et al., 2010)	0,61	0,04	NiO $InTaO_4$ (Z.Y. Wang et al., 2010)		2,8
NT/Cu-600 (Varghese et al., 2009)	2,84		CoPc TiO_2 (Zhao et al. 2009)		9,3

Table 3.2. Photocatalytic carbon dioxide reduction rates from literature

3.1 Catalytic vs photocatalytic CO$_2$ reduction

A microkinetic analysis for catalytic CO$_2$ hydrogenation on Cu (111) surface was performed in order to reveal catalytic rates at ambient conditions and also to study the effect of water in carbon dioxide reduction mechanism. The microkinetic analysis was expected to reveal rate determining steps in photocatalytic carbon dioxide reduction based on the assumption of similar reaction mechanism with catalytic hydrogenation since both processes involve copper based catalysts for methanol production.

In photocatalytic carbon dioxide reduction mechanism, whether every step in the mechanism is light activated or not is still ambiguous. One consensus could be the carbon dioxide activation to be the essential step for reduction (Solymosi & Tombacz, 1994). But after CO$_2$ activation, reduction could proceed catalytically.

Presence of catalytic steps in CO$_2$ hydrogenation in artificial photocatalysis (just like in photosynthesis) was suggested based on the observations from literature such as temperature sensitivity of the photocatalytic CO$_2$ reduction (Chen et al., 2009, Zhang et al., 2009, Z.Y. Wang et al., 2010) and realization of reduction without light illumination at room conditions (Varghese et al. 2009).

In the microkinetic analysis, the mechanism was selected to include water gas shift reaction together with the carbon dioxide hydrogenation since carbon monoxide and carbon dioxide were simultaneously used in industry for better methanol production rates.

$$CO_2 + 3H_2 \leftrightarrow CH_3OH + H_2O$$

$$CO + H_2O \leftrightarrow CO_2 + H_2$$
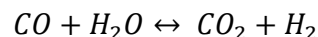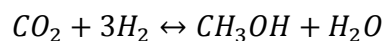
The reaction mechanism could be seen in Table 3.3.

Steps	Reactions
1	$5/H_2 + * \leftrightarrow H_2 *$
2	$5/H_2 * + * \leftrightarrow 2H *$
3	$CO_2 + * \leftrightarrow CO_2 *$
4	$CO + * \leftrightarrow CO *$
5	$CO * + O * \leftrightarrow CO_2 * + *$
6	$2/CO_2 * + H * \leftrightarrow HCOO * + *$
7	$2/HCOO * + H * \leftrightarrow H_2CO * + O *$
8	$2/H_2CO * + H * \leftrightarrow H_3CO * + *$
9	$2/H_3CO * + H * \leftrightarrow H_3COH * + *$
10	$2/CH_3OH * \leftrightarrow CH_3OH + *$
11	$O * + H * \leftrightarrow OH * + *$
12	$OH * + H * \leftrightarrow H_2O * + *$
13	$H_2O * \leftrightarrow H_2O + *$
Total	$CO_2 + CO + 5H_2 \leftrightarrow 2CH_3OH + H_2O$

Table 3.3. Elementary reaction steps used in the microkinetic modeling

Enthalpy changes of reaction steps and individual activation energy barriers were calculated using Bond Order Conservation – Morse Potential Method as proposed by Shustorovic & Bell, 1991. In this method, enthalpy changes of the reaction steps were calculated from heats of chemisorptions of surface species on Cu (111) surface and from bond energies (Table 3.4). In the calculation of the pre-exponential factors of the reaction steps, one of the pre-exponential factors is estimated from transition state theory (Dumesic et al., 1993) and the other was calculated accordingly from the entropy change of that elementary step. The entropy change values of the elementary steps were calculated from partition functions of surface intermediates.

$$\frac{Af}{Ar} = \frac{z_C z_D}{z_A z_B} = exp\left(\frac{\Delta S^0}{R}\right) \ for \ the \ reaction \ A + B \rightarrow C + D \tag{2}$$

$k_f = A_f * exp(-E_{af}/RT)$			$k_r = A_r * exp(-E_{ar}/RT)$	
A^r (s^{-1} or bar^{-1}s^{-1})	E_{af} (kJ/mol)	**Reactions**	A^r (s^{-1} or bar^{-1}s^{-1})	E_{ar} (kJ/mol)
$6.77*10^5$	0	$H_2 + * \leftrightarrow H_2 *$	$6*10^{12}$	21
$1*10^{13}$	52.5	$H_2 * + * \leftrightarrow 2H *$	$8.55*10^{12}$	64.5
$1*10^6$	0	$CO_2 + * \leftrightarrow CO_2 *$	$1.62*10^{13}$	21
$1*10^6$	0	$CO + * \leftrightarrow CO *$	$8.86*10^{14}$	50
$1*10^{13}$	44.8	$CO * + O * \leftrightarrow CO_2 * + *$	$2.38*10^{13}$	115.8
$1*10^{13}$	14	$CO_2 * + H * \leftrightarrow HCOO * + *$	$1.79*10^{11}$	6
$1*10^{13}$	79	$HCOO * + H * \leftrightarrow H_2CO * + O *$	$1*10^{13}$	0
$1*10^{13}$	15.5	$H_2CO * + H * \leftrightarrow H_3CO * + *$	$1*10^{13}$	36.5
$1*10^{13}$	41	$H_3CO * + H * \leftrightarrow H_3COH * + *$	$1.06*10^{14}$	75
$9*10^{16}$	63	$CH_3OH * \leftrightarrow CH_3OH + *$	$1*10^6$	0
$1*10^{13}$	86.8	$O * + H * \leftrightarrow OH * + *$	$5.31*10^{11}$	64.8
$1*10^{13}$	6	$OH * + H * \leftrightarrow H_2O * + *$	$9.78*10^{14}$	107
$1.59*10^{14}$	59	$H_2O * \leftrightarrow H_2O + *$	$1*10^6$	0

Table 3.4. Used energy barriers and pre exponential factors in microkinetic modeling

In the microkinetic analysis, coverage trends of the surface intermediates can be easily followed with given individual rate constants. For an initial gas composition of %70 H_2, %25 CO and %5 CO_2, surface coverage trends of CO_2, CO and H at industrial conditions can be seen in Figure 3.1 for a time interval of 0- 10^{-7} s.

From Figure 3.1, it was observed that CO and CO_2 adsorbs and saturates on the surface as soon as 10^{-10}s. However, adsorption of H species controls the vacant site which is dominant in the mechanism.

Effect of water on the catalytic methanol formation rates were studied by changing the initial gas composition to 70 % H_2, 24 % CO, 4 % CO_2, 2% H_2O from 70 % H_2, 25 % CO, 5 % CO_2. The results were shown for a carbon dioxide conversion of 0.00005 at industrial conditions and also at ambient conditions in order to compare with industrial and photocatalytic rates (Table 3.5).

The validity of the microkinetic analysis results was verified with the comparison of the methanol formation rate with literature value (Sahibzada et al., 1998). The inhibitory effect of water on catalytic carbon dioxide hydrogenation mechanism is observed especially at low

temperatures. Positive effect of pressure on carbon dioxide reduction rates was also observed with this microkinetic analysis.
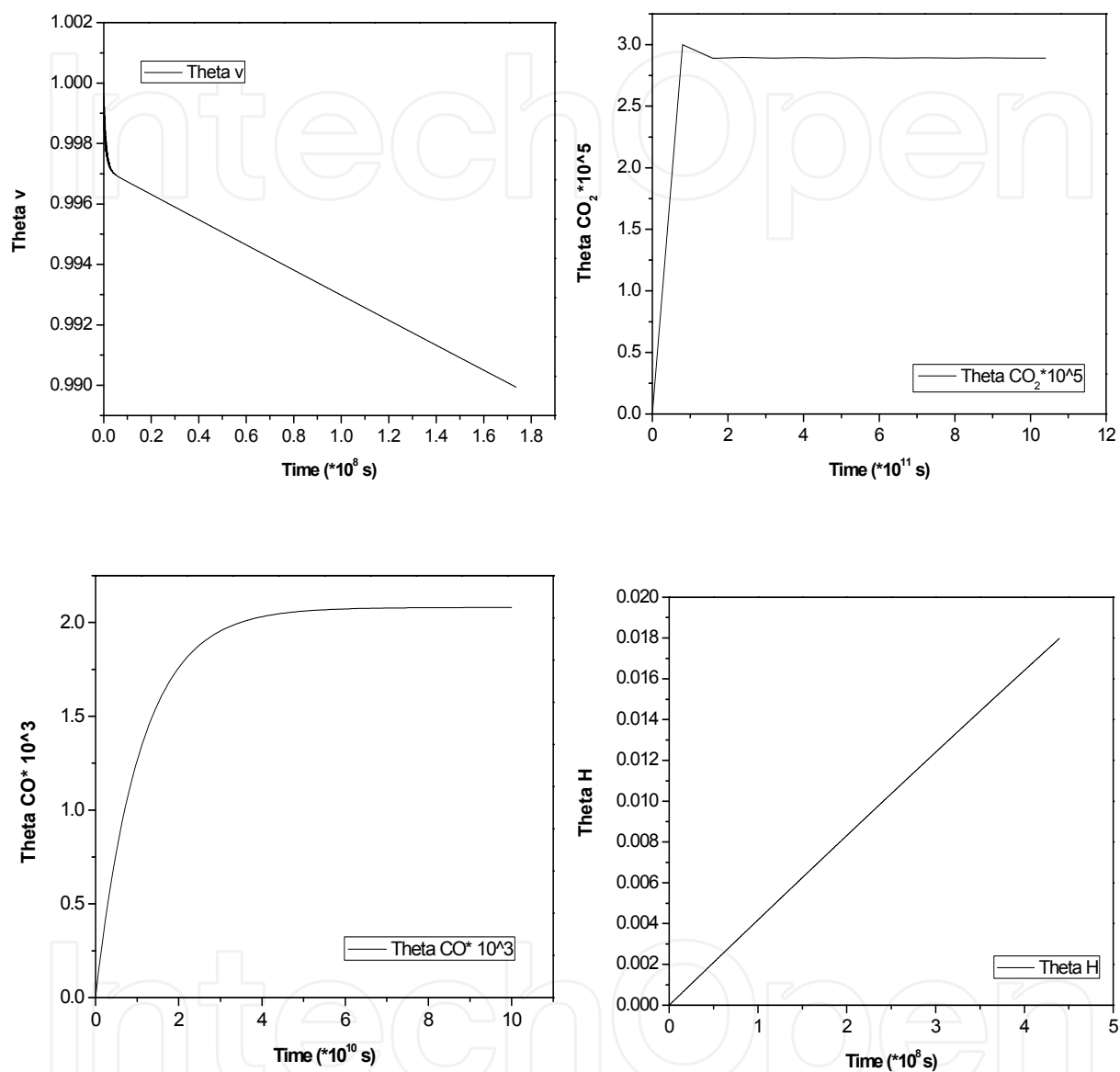

Fig. 3.1. Coverage values of vacant sites, CO, CO_2 and H at 75 bar and 523 K

When the catalytic methanol formation rates were compared with photocatalytic rates, it is seen that at room conditions; i.e., at 300 K and 1 atm, photocatalytic rates (20 μmol/g_{cat}/h ~6*10^{-9} mol/gcat/s (Tseng et al., 2002)) significantly surpass catalytic rates (2.07*10^{-12} mol/gcat/s). Even though estimation of kinetic parameters could contribute to non certainty of the kinetic results, it could be observed from the comparison that photo irradiation results in an obvious improvement in methanol formation rates. This improvement could be attributed to easier activation of molecules such as carbon dioxide through transfer of a photo-generated electron.

Reaction Conditions	Microkinetic Modeling		Literature
	Without initial H₂O	With initial H₂O	
523 K 75 bar	$4.53*10^{-5}$	$3.58*10^{-5}$	$6.1*10^{-5}$ (with $Cu/ZnO/Al_2O_3$) (Sahibzada et al., 1998)
300 K 75 bar	$1.07*10^{-9}$	$4.58*10^{-12}$	
300 K 1 bar	$1.9*10^{-11}$	$2.07*10^{-12}$	Photocatalytic: $6*10^{-9}$ (with Cu/TiO_2) (Tseng et al., 2002)

Table 3.5. Methanol formation rates (mol/g_cat/s) at different reaction conditions with or without initial water concentration

3.2 Rate determining step of methanol formation on Cu (111) surface

Calculation of degree of rate controls for elementary reaction steps in the microkinetic model allows revealing rate limiting steps in methanol formation from CO_2 hydrogenation and water gas shift reaction. Degree of rate control is defined by Campbell such as; the degree of change of the overall rate by a change in rate constant of a single step (Equation 2) (Campbell, 2001). Campbell proposed that steps where degree of rate control is positive be called rate-limiting steps and negative be inhibition steps. The larger the numeric value of degree of rate control, $X_{rc,i}$, the bigger is the influence of its rate constant on the overall reaction rate.

$$X_{rc,i} = (k_i/\delta k_i)*(\delta R/R) \quad\quad (3)$$

When degree of rate control values were calculated for the microkinetic model of methanol synthesis on Cu (111) surface, the results indicated that H supply (Step 2) to Cu surface as well as formate hydrogenation step (step 7) is essential especially at 300 K, at which artificial photosynthesis occurs (Table 3.6). This study underlines the importance of H supply and

	Elementary reactions	$X_{rc,i}$			
		75 atm 523 K	75 atm 423 K	75 atm 300 K	1 atm 300K
1	$H_2 + * \leftrightarrow H_2 *$	~0	0	0	0
2	$H_2 * + * \leftrightarrow 2H *$	0.36	2.4	3.53	3.7
3	$CO_2 + * \leftrightarrow CO_2 *$	0	0	~0	0
4	$CO + * \leftrightarrow CO *$	0	0	-3.67	-0.21
5	$CO * + O * \leftrightarrow CO_2 * + *$	0	0	0	0
6	$CO_2 * + H * \leftrightarrow HCOO * + *$	0	0	0	0
7	$HCOO * + H * \leftrightarrow H_2CO * + O *$	0.997	~1	~1	1
8	$H_2CO * + H * \leftrightarrow H_3CO * + *$	~0	~0	0.71	0.57
9	$H_3CO * + H * \leftrightarrow H_3COH * + *$	0	0.56	~1	1
10	$CH_3OH * \leftrightarrow CH_3OH + *$	-	-	-	-
11	$O * + H * \leftrightarrow OH * + *$	0	0	0	0
12	$OH * + H * \leftrightarrow H_2O * + *$	0	0	0	0
13	$H_2O * \leftrightarrow H_2O + *$	0	0	0	0

Table 3.6. The degree of rate control values with respect to r_f10 ($CH_3OH * \leftrightarrow CH_3OH + *$) found by finite difference method at t= $5.18*10^{-7}$ s

concentration on the surface for methanol formation rates. Since water splitting reaction is the only source of H in photocatalytic CO_2 reduction mechanism, it could be said that water oxidation rates are rate limiting in artificial photosynthesis systems whereas water oxidation rate surpass carbon dioxide reduction rates at photosynthesis (Table 2.1).

4. Similarities and differences between photosynthesis and artificial photosynthesis

Analogy between photosynthesis and artificial photosynthesis is in the similar tools and methods utilized in both systems. Collecting solar energy for triggering chemical reactions by chlorophyll pigments packed in thylakoid membrane or by semiconductors; oxidizing water into molecular oxygen and protons and reducing CO_2 with transported electrons and H^+s are among the similarities of the two systems. However, the gap between the design of the systems and number of reaction sites and intermediate molecules result in more sophisticated and simpler products in photosynthesis ($(CH_2O)_6$) and in photocatalysis (CH_4 or CH_3OH) respectively.

In photosynthesis, there are three major reaction centers in light dependent reactions, regulating electron and proton transport together with the intermediate charge carriers (redox components). In photocatalysis, on the other hand, design of the system is limited to the presence of a pool of charges wandering on the semiconductor/metal surface in an unregulated fashion, increasing the chance of recombination of charge carriers. In addition, realization of oxidation and reduction reactions on the same catalyst surface results in interactions between the surface adsorbates which is proven to be inhibitory on reaction rates as studied with the microkinetic model in Section 3.1.

In photosynthesis, CO_2 diffusion from atmosphere to stromal phase in chloroplasts is controlled by stomata activities and permeability of chloroplast membranes. Photosynthetic rate is limited with the CO_2 concentration in stromal phase for values lower than a saturation value; i.e., the photosynthetic rate is linearly increasing with CO_2 concentration. For CO_2 concentrations above the saturation value, photosynthetic rate stays constant, limited by the rate of the enzyme system. Since CO_2 concentration in the stromal phase is related to CO_2 diffusion, photosynthetic rate is dependent upon diffusion rates.

In photocatalysis, diffusion of dissolved CO_2 and other reactants/products to/from the catalyst surface is largely dependent upon the reactor types, reaction media and stirring rates. The photocatalytic experiment parameters are not standardized in literature, resulting in confusion about the proper comparison of the real kinetic data. For photocatalytic tests performed in liquid media, which constitute the majority of the tests reported in literature, presence of gas-liquid-solid interfaces imposes non negligible mass transfer limitations in observed rates. A study performed to reveal the effect of stirring rates on photocatalytic hydrogen evolution rates indicated the importance of boundary layer and gas-liquid equilibrium in liquid phase photocatalytic experiments (Figure 4.1) (Ipek, 2011).

Increase in photo catalytic rates with increasing stirring rates (from 350 rpm to 900 rpm) up to a certain hydrogen concentration could be interpreted as decreased mass transfer limitation effects due to thinning of the boundary layer surrounding the catalyst particles whereas after that concentration, hydrogen seems to accumulate in the gas phase with the same limiting liquid-gas transfer rate. The limitation at the gas-liquid interface could also be inferred from the overlapping hydrogen amounts accumulated in the gas phase regardless of the catalyst amount or the reaction mixture volume (Figure 4.2).
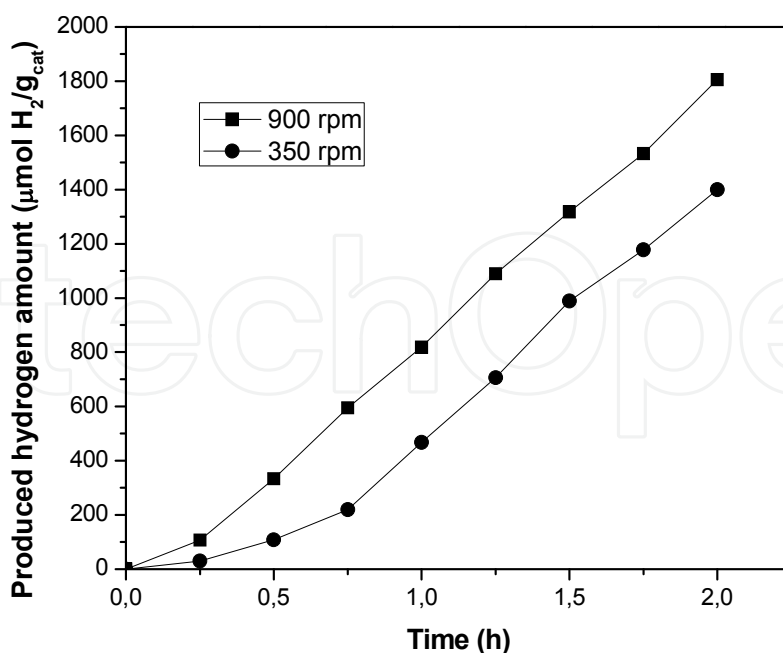
Fig. 4.1. Effect of stirring rates on photocatalytic hydrogen evolution with methanol as sacrificial agent, with 0.5 wt % Pt/TiO_2, 250 ml deionized water, 2 ml methanol (■) 900 rpm, (●) 350 rpm
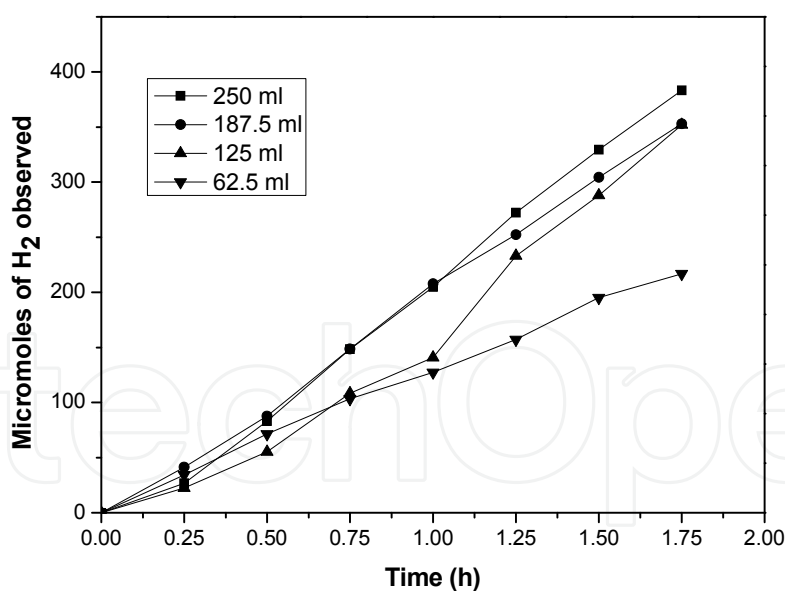

Fig. 4.2. Observed hydrogen amount in the gas phase with changing reaction mixture, (■) 62.5 ml (●) 125 ml (▲) 187.5 ml (▼) 250 ml, CH_3OH/H_2O: 1/125 (v/v) and C_{cat}: 1 g/L for each case

Furthermore, temperature sensitivity of the photocatalytic hydrogen evolution reactions indicate presence of diffusion limitations with found 12 and 19.5 kJ/mol apparent activation energies for Pt/TiO_2 and Cu/TiO_2 reactions respectively (Ipek, 2011).

In PSII of photosynthesis, there are over 15 polypeptides and 9 different redox components responsible for water oxidation and electron transport. Even the oxygen evolving complex is regenerating itself at every 30 minutes in order to sustain its stability. Along with the sophistication of light dependent reactions including numerous intermediate charge carriers, difference in the CO_2 reduction mechanism (activating CO_2 by fixing it into another chemical) with 13 specific enzymes result in higher photosynthetic rates and more complicated products (such as glucose) in photosynthesis. On the other hand, C-C bond making is still remaining as a challenge in artificial photosynthesis systems. Even with one carbon chemical synthesis, photocatalytic rates are well below photosynthetic rates. To illustrate, CO_2 reduction using titanium nanotubes resulted in nearly 1 nmol/m^2/s CH_4 production rate (Schulte et al., 2010) whereas an avarage photosynthetic rate is 12 μmol/m^2/s.

Apart from the sophisticated numerous enzymes taking part in carbon dioxide reduction mechanism, the major gap between carbon dioxide reduction rates are suggested to result from undeveloped charge and H transport systems in artificial photosynthesis systems. Recently, regulated electron and hole transport is reported with zeolites increasing the charge separation and water oxidation activity (Dutta & Severance, 2011). Furthermore, H^+ transport through oxidation center to the reduction center is reported to be realized with H^+ permeable electron conducting membrane (Hou et al., 2011). Design of a reaction system as well as the photocatalyst is of uttermost importance in artificial photosynthesis systems for better activities. As indicated in the microkinetic analysis part, carbon dioxide reduction rates mainly suffer from insufficient H supply to the reduction centers at artificial photosynthesis. In photosynthesis, H transport is highly regulated via the intermediate charge carriers such as NADP+ and via the electrochemical potential difference which may be attributed to the presence of an interstitial membrane. Utilization of such a membrane in photocatalytic systems was first suggested by Kitano et al., 2007b who used the membrane for H transport in water splitting reaction. Similarly, enhanced electron and H transport system should be implemented for carbon dioxide reduction also which would carry the artificial photosynthesis systems to industrial levels.
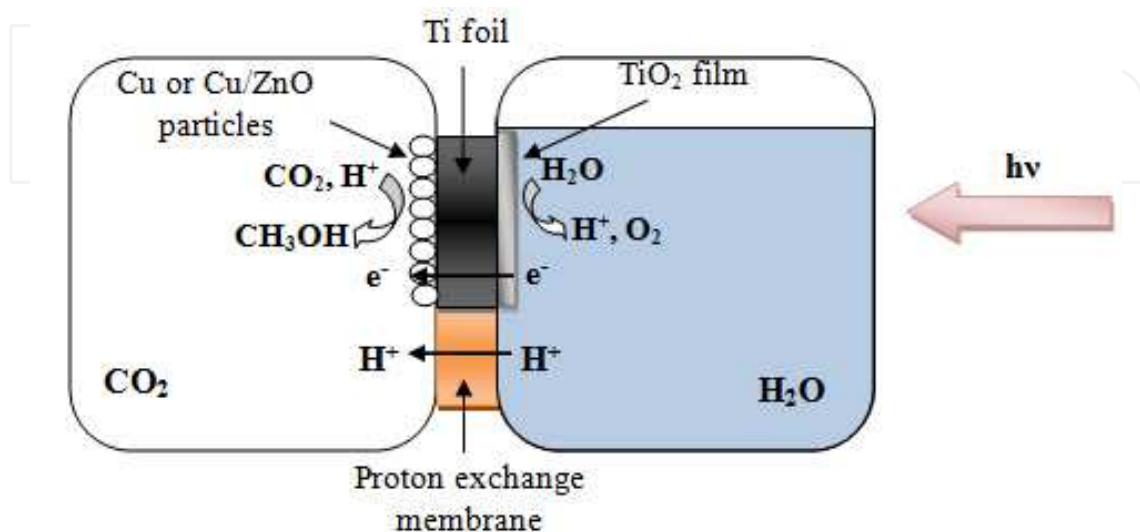

Fig. 4.3. Schematic illustration of suggested reactor for CO_2 reduction

Design of a photocatalytic reactor would work in such a way that in one compartment light is harvested by the semiconductor in order to split water to form H^+s and by the transfer of produced protons and electrons, CO_2 could be reduced with another catalyst, such as copper, in the other compartment. In this way, with the help of proton exchange membranes and separate reaction centers, interaction between reactants or products and therefore reverse reactions could be prevented by supplying Hs to catalytic compartment at the same time. On the other hand, a high conductance electron membrane would prevent charge recombination as illustrated in Figure 4.3.

Such a system has already been proposed by Kitano et al. (2007b) for water splitting reaction. Introducing CO_2 in the picture will be the next generation modification of the artificial photosynthesis systems. Further refinement of the design will be possible with more understanding about the rates of chemical conversions and the rates of transport.

5. Conclusions

Photosynthesis and artificial photosynthesis system were compared in this study with an emphasis on charge and H transport which is indicated to be the main reason for the difference in resulting carbon dioxide reduction yields and rates. The gap in artificial systems was found to be in the design of the photocatalytic systems which could be developed with a membrane which would enhance charge separation and H transport. H supply to carbon dioxide reduction centers were found to be limiting the existing photocatalytic carbon dioxide reduction rates, indicating the important role of water splitting in artificial photosynthesis systems. Water being in contact with carbon dioxide on photocatalyst surface was found to act negatively on the methanol formation rates by inhibiting carbon dioxide activation. For a better carbon dioxide reduction with existing photocatalysts, separation of the reaction centers was proposed which would enhance the charge and H transport at the same time.

6. Acknowledgements

7. References

Anpo, M. & Chiba, K. (1992). Photocatalytic Reduction of CO_2 on Anchored Titanium-Oxide Catalysts, *7th International Symposium on Relations between Homogeneous and Heterogeneous Catalysis*, ISBN 0304-5102, Tokyo, Japan, May 1992

Anpo, M.; Yamashita, H.; Ichihashi, Y. & Ehara, S. (1995). Photocatalytic Reduction of CO_2 with H_2O on Various Titanium-Oxide Catalysts. *Journal of Electroanalytical Chemistry*, Vol. 396, No. 1-2, pp. 21-26, ISSN 0022-0728

Anpo, M.; Yamashita, H.; Ichihashi, Y.; Fujii, Y. & Honda, M. (1997). Photocatalytic Reduction of CO_2 with H_2O on Titanium Oxides Anchored within Micropores of Zeolites: Effects of the Structure of the Active Sites and the Addition of Pt. *Journal of Physical Chemistry B*, Vol. 101, No. 14, pp. 2632-2636, ISSN 1089-5647

Anpo, M.; Yamashita, H.; Ikeue, K.; Fujii, Y.; Zhang, S. G.; Ichihashi, Y.; Park, D. R.; Suzuki, Y.; Koyano, K. & Tatsumi, T. (1998). Photocatalytic Reduction of CO_2 with H_2O on Ti-MCM-41 and Ti-MCM-48 Mesoporous Zeolite Catalysts. *Catalysis Today*, Vol. 44, No. 1-4, pp. 327-332, ISSN 0920-5861

Asahi, R.; Morikawa, T.; Ohwaki, T.; Aoki, K. & Taga, Y. (2001). Visible-Light Photocatalysis in Nitrogen-Doped Titanium Oxides. *Science*, Vol. 293, No. 5528, pp. 269-271 ISSN 0036-8075

Campbell, C. T. (2001). Finding the Rate-Determining Step in a Mechanism - Comparing Dedonder Relations with the "Degree of Rate Control". *Journal of Catalysis*, Vol. 204, No. 2, pp. 520-524, ISSN 0021-9517

Carp, O.; Huisman, C. L. & Reller, A. (2004). Photoinduced Reactivity of Titanium Dioxide. *Progress in Solid State Chemistry*, Vol. 32, No. 1-2, pp. 33-177, ISSN 0079-6786

Chen, L.; Graham, M. E.; Li, G. H.; Gentner, D. R.; Dimitrijevic, N. M. & Gray, K. A. (2009). Photoreduction of CO_2 by TiO_2 Nanocomposites Synthesized through Reactive Direct Current Magnetron Sputter Deposition. *Thin Solid Films*, Vol. 517, No. 19, pp. 5641-5645, ISSN 0040-6090

Dey, G. R.; Belapurkar, A. D. & Kishore, K. (2004). Photo-Catalytic Reduction of Carbon Dioxide to Methane using TiO_2 as Suspension in Water. *Journal of Photochemistry and Photobiology a-Chemistry*, Vol. 163, No. 3, pp. 503-508, ISSN 1010-6030

Diwan, J. J. (January, 2009). Calvin Cycle- Photosynthetic Dark Reactions, In: *Rensselaer Polytechnic Institute*, 27.03.2011, Available from http://www.rpi.edu/dept/bcbp/molbiochem/ MBWeb/mb2/part1/dark.htm

Dutta, P. K. & Severance, M. (2011). Photoelectron Transfer in Zeolite Cages and Its Relevance to Solar Energy Conversion. *Journal of Physical Chemistry Letters*, Vol. 2, No. 5, (March 2011), pp. 467-476, ISSN 1948- 7185

Freund, H. J. & Roberts, M. W. (1996). Surface Chemistry of Carbon Dioxide. *Surface Science Reports*, Vol. 25, No. 8, pp. 225-273, ISSN 0167-5729

Govindjee, (Ed.). (1975). *Bioenergetics of Photosynthesis*, Academic Press, ISBN, New York

Hankamer, B.; Barber, J. & Boekema, E. J. (1997). Structure and Membrane Organization of Photosystem II in Green Plants. *Annual Review of Plant Physiology and Plant Molecular Biology*, Vol. 48, pp. 641-671, ISSN 1040- 2519

Haumann, M.; Liebisch, P.; Muller, C.; Barra, M.; Grabolle, M. & Dau, H. (2005). Photosynthetic O-2 Formation Tracked by Time-Resolved X-ray Experiments. *Science*, Vol. 310, No. 5750, (November 2005), pp. 1019-1021, ISSN 0036- 8075

Heldt, H. W.; Piechulla B. & Heldt, F. (Eds.). (2010). *Plant Biochemistry*, Elsevier Science & Technology, ISBN 9780123849861, London, 4th Edition.

Hill, R. & Bendall, F. (1960). Function of the Two Cytochrome Components in Chloroplasts: A Working Hypothesis. *Nature*, Vol. 186, No. 4719, pp. 136-137, ISSN 0028-0836

Hou, Y.; Abrams, B.L.; Vesborg, P.C.K.; Bjorketan, H.E.; Herbst, K.; Bech, L.; Setti, A.M.; Damsgaard, C.D.; Redersen, T.; Hansen, O.; Rossmeisl, J.; Dahl, S.; Norskov, J.K. & Chorkendorff, I. (2011). Bioinspired Molecular co-Catalysts Bonded to a Silicon Photocathode for Solar Hydrogen Evolution. *Nature Materials*, Vol. 10, pp. 434-438, ISSN 1476-1122

Hwang, J. S.; Chang, J. S.; Park, S. E.; Ikeue, K. & Anpo, M. (2005). Photoreduction of Carbondioxide on Surface Functionalized Nanoporous Catalysts. *Topics in Catalysis*, Vol. 35, No. 3-4, (July 2005), pp. 311-319, ISSN 1022-5528

Indrakanti, V. P.; Schobert, H. H. & Kubicki, J. D. (2009). Quantum Mechanical Modeling of CO_2 Interactions with Irradiated Stoichiometric and Oxygen-Deficient Anatase TiO_2 Surfaces: Implications for the Photocatalytic Reduction of CO_2. *Energy & Fuels*, Vol. 23, (October 2009), pp. 5247-5256, ISSN 0887- 0624

Inoue, T.; Fujishima, A.; Konishi, S. & Honda, K. (1979). Photoelectrocatalytic Reduction of Carbon-Dioxide in Aqueous Suspensions of Semiconductor Powders. *Nature*, Vol. 277, No. 5698, pp. 637-638, ISSN 0028-0836

Ipek, B. (April 2011). Photocatalytic Carbon Dioxide Reduction in Liquid Media. M.Sc. Thesis, Chemical Engineering Department, Middle East Technical University, Ankara, Turkey

Jitaru, M. (2007). Electrochemical Carbon Dioxide Reduction- Fundamental and Applied Topics (Review). *Journal of the University of Chemical Technology and Metallurgy*, Vol. 42, No. 4, pp. 333-344, ISSN 1311-7629

Kaneco, S.; Shimizu, Y.; Ohta, K. & Mizuno, T. (1998). Photocatalytic Reduction of High Pressure Carbon Dioxide using TiO_2 Powders with a Positive Hole Scavenger. *Journal of Photochemistry and Photobiology a-Chemistry*, Vol. 115, No. 3, pp. 223-226, ISSN 1010-6030

Ke, B. (2001). *Photosynthesis: Photobiochemistry and Photobiophysics*, Kluwer Academic Publishers, ISBN 0-7923-6334-5, Dordrecht

Kitano, M.; Matsuoka, M.; Ueshima, M. & Anpo, M. (2007a). Recent Developments in Titanium Oxide-Based Photocatalysts. *Applied Catalysis a-General*, Vol. 325, No. 1, pp. 1-14, ISSN 0926- 860X

Kitano, M.; Takeuchi, M.; Matsuoka, M.; Thomas, J. A. & Anpo, M. (2007b). Photocatalytic Water Splitting using Pt-Loaded Visible Light-Responsive TiO_2 Thin Film Photocatalysts. *Catalysis Today*, Vol. 120, No. 2, pp. 133-138, ISSN 0920-5861

Koci, K.; Mateju, K.; Obalova, L.; Krejcikova, S.; Lacny, Z.; Placha, D.; Capek, L.; Hospodkova, A.; & Solcova, O. (2010). Effect Of Silver Doping on The TiO_2 for Photocatalytic Reduction of CO_2. *Applied Catalysis B-Environmental*, Vol. 96, No. 3-4, pp. 239-244, ISSN 0926-3373

Koci, K.; Obalova, L.; Matejova, L.; Placha, D.; Lacny, Z.; Jirkovsky, J. & Solcova, O. (2009). Effect of TiO_2 Particle Size on the Photocatalytic Reduction of CO_2. *Applied Catalysis B-Environmental*, Vol. 89, No. 3-4, pp. 494-502, ISSN 0926-3373

Meyer, T. J. (2008). Catalysis - The Art of Splitting Water. *Nature*, Vol. 451, No. 7180, pp. 778-779, ISSN 0028-0836

Ovesen, C. V.; Clausen, B. S.; Schiotz, J.; Stoltze, P.; Topsoe, H. & Norskov, J. K. (1997). Kinetic Implications of Dynamical Changes in Catalyst Morphology During Methanol Synthesis over Cu/ZnO Catalysts. *Journal of Catalysis*, Vol. 168, No. 2, pp. 133-142, ISSN 0021- 9517

Ozcan, O.; Yukruk, F.; Akkaya, E. U. & Uner, D. (2007). Dye Sensitized Artificial Photosynthesis in the Gas Phase over Thin and Thick TiO_2 Films under UV and Visible Light Irradiation. *Applied Catalysis B-Environmental*, Vol. 71, No. 3-4, pp. 291-297, ISSN 0926-3373

Sahibzada, M.; Metcalfe, I. S. & Chadwick, D. (1998). Methanol Synthesis from $CO/CO_2/H_2$ over $Cu/ZnO/Al_2O_3$ at Differential and Finite Conversions. *Journal of Catalysis*, Vol. 174, No. 2, pp. 111-118, ISSN 0021- 9517

Schulte, K. L.; DeSario, P. A. & Gray, K. A. (2010). Effect of Crystal Phase Composition on the Reductive and Oxidative Abilities of TiO_2 Nanotubes under UV and Visible Light. *Applied Catalysis B-Environmental*, Vol. 97, No. 3-4, pp. 354-360, ISSN 0926-3373

Shustorovich, E. & Bell, A. T. (1991). An Analysis of Methanol Synthesis from CO and CO_2 on Cu and Pd Surfaces by the Bond-Order-Conservation Morse-Potential Approach. *Surface Science*, Vol. 253, No. 1-3, pp. 386-394, ISSN 0039-6028

Singal, H. R.; Talwar, G.; Dua, A. & Singh, R. (1995). Pod Photosynthesis and Seed Dark CO_2 Fixation Support Oil Synthesis in Developing Brassica Seeds. *Journal of Biosciences*, Vol. 20, No. 1, pp. 49-58, ISSN 0250-5991

Solymosi, F. & Tombacz, I. (1994). Photocatalytic Reaction of H_2O+CO_2 over Pure and Doped Rh/TiO_2. *Catalysis Letters*, Vol. 27, No. 1-2, pp. 61-65, ISSN 1011-372X

Tseng, I. H.; Chang, W. C. & Wu, J. C. S. (2002). Photoreduction of CO_2 using Sol-Gel Derived Titania and Titania-Supported Copper Catalysts. *Applied Catalysis B-Environmental*, Vol. 37, No. 1, pp. 37-48, ISSN 0926-3373

Umena, Y.; Kawakami, K.; Shen, J. R. & Kamiya, N. (2011). Crystal Structure of Oxygen-Evolving Photosystem II at a Resolution of 1.9 A. Nature, Vol. 473, No. 7345, pp. 55-60, ISSN 0028-0836

Uner, D.; Oymak, M. M. & Ipek, B. (2011). CO_2 Utilization by Photocatalytic Conversion to Methane and Methanol. *International Journal of Global Warming*, Vol. 3, No. 1-2, pp. 142-162, ISSN 1758-2083

VandenBussche, K. M. & Froment, G. F. (1996). A Steady-State Kinetic Model for Methanol Synthesis and the Water Gas Shift Reaction on a Commercial $Cu/ZnO/Al_2O_3$ Catalyst. *Journal of Catalysis*, Vol. 161, No. 1, pp. 1-10, ISSN 0021-9517

Varghese, O. K.; Paulose, M.; LaTempa, T. J. & Grimes, C. A. (2009). High-Rate Solar Photocatalytic Conversion of CO_2 and Water Vapor to Hydrocarbon Fuels. *Nano Letters*, Vol. 9, No. 2, pp. 731-737, ISSN 1530-6984

Wang, C. J.; Thompson, R. L.; Baltrus, J. & Matranga, C. (2010). Visible Light Photoreduction of CO_2 Using $CdSe/Pt/TiO_2$ Heterostructured Catalysts. *Journal of Physical Chemistry Letters*, Vol. 1, No. 1, pp. 48-53, ISSN 1948-7185

Wang, Z. Y.; Chou, H. C.; Wu, J. C. S.; Tsai, D. P. & Mul, G. (2010). CO_2 Photoreduction using $NiO/InTaO_4$ in Optical-Fiber Reactor for Renewable Energy. *Applied Catalysis a-General*, Vol. 380, No. 1-2, pp. 172-177, ISSN 0926-860X

Whitmarsh, J.; Govindjee (1999). The Photosynthetic Process, In: *Concepts in Photobiology: Photosynthesis and Photomorphogenesis,* Singhal, G.S.; Renger, G.; Sopory, S. K.; Irrgang, K. D. & Govindjee, Narosa Publishing House, ISBN 0-7923-5519-9, New Delhi

Whittingham, C. P. (1974). *The Mechanism of Photosynthesis*, American Elsevier Pub. Co, ISBN 9780444195524 , New York

Woan, K.; Pyrgiotakis, G. & Sigmund, W. (2009). Photocatalytic Carbon-Nanotube-TiO_2 Composites. *Advanced Materials*, Vol. 21, No. 21, pp. 2233-2239, ISSN 0935-9648

Wu, J. C. S.; Lin, H. M. & Lai, C. L. (2005). Photo Reduction of CO_2 to Methanol using Optical-Fiber Photoreactor. *Applied Catalysis a-General*, Vol. 296, No. 2, pp. 194-200, 0926-860X

Yamashita, H.; Nishiguchi, H.; Kamada, N.; Anpo, M.; Teraoka, Y.; Hatano, H.; Ehara, S.; Kikui, K.; Palmisano, L.; Sclafani, A.; Schiavello, M. & Fox, M. A. (1994).

Photocatalytic Reduction of CO_2 with H_2O on TiO_2 and Cu/TiO_2 Catalysts. *Research on Chemical Intermediates*, Vol. 20, No. 8, pp. 815-823, ISSN 0922-6168

Yang, H. C.; Lin, H. Y.; Chien, Y. S.; Wu, J. C. S. & Wu, H. H. (2009), Mesoporous TiO_2/SBA-15 and Cu/TiO_2/SBA-15 Composite Photocatalysts for Photoreduction of CO_2 to Methanol. *Catalysis Letters*, Vol. 131, No. 3-4, pp. 381-387, ISSN 1011-372X

Zhang, Q. H.; Han, W. D.; Hong, Y. J. & Yu, J. G. (2009). Photocatalytic Reduction of CO_2 with H_2O on Pt-loaded TiO_2 Catalyst. *Catalysis Today*, Vol. 148, No. 3-4, pp. 335-340, ISSN 0920-5861

Zhao, Z. H.; Fan, J. M.; Xie, M. M. & Wang, Z. Z. (2009). Photo-Catalytic Reduction of Carbon Dioxide with in-situ Synthesized $CoPc/TiO_2$ under Visible Light Irradiation. *Journal of Cleaner Production*, Vol. 17, No. 11, pp. 1025-1029, ISSN 0959-6526
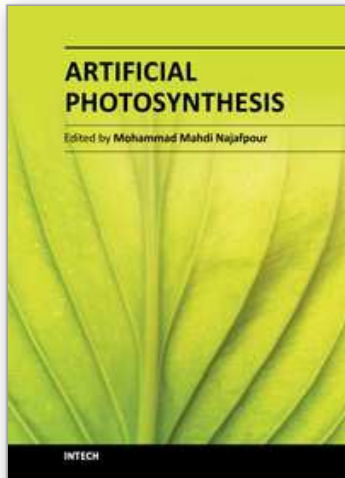
Artificial Photosynthesis

Edited by Dr Mohammad Najafpour

Photosynthesis is one of the most important reactions on Earth, and it is a scientific field that is intrinsically interdisciplinary, with many research groups examining it. We could learn many strategies from photosynthesis and can apply these strategies in artificial photosynthesis. Artificial photosynthesis is a research field that attempts to replicate the natural process of photosynthesis. The goal of artificial photosynthesis is to use the energy of the sun to make different useful material or high-energy chemicals for energy production. This book is aimed at providing fundamental and applied aspects of artificial photosynthesis. In each section, important topics in the subject are discussed and reviewed by experts.

How to reference

In order to correctly reference this scholarly work, feel free to copy and paste the following:

Bahar Ipek and Deniz Uner (2012). Artificial Photosynthesis from a Chemical Engineering Perspective, Artificial Photosynthesis, Dr Mohammad Najafpour (Ed.), ISBN: 978-953-307-966-0, InTech, Available from: http://www.intechopen.com/books/artificial-photosynthesis/artificial-photosynthesis-from-a-chemical-engineering-perspective

INTECH
open science | open minds